



1 **Development and performance of a high-resolution surface wave and storm surge forecast model**
2 **(COASTLINES-LO): Application to a large lake**

3 **Laura L. Swatridge¹, Ryan P. Mulligan¹, Leon Boegman¹, and Shiliang Shan²**

4 ¹ Department of Civil Engineering, Queen's University, Kingston, ON, Canada, K7L 3N6.

5 ² Department of Physics and Space Science, Royal Military College of Canada, Kingston, ON, Canada,
6 K7K 7B4.

7 Correspondence to: Laura Swatridge (l.swatridge@queensu.ca)

8

9 **Key Points:**

- 10 • A real-time forecast model of wind-driven hydrodynamics in Lake Ontario is developed.
- 11 • Model performance compares well with observed data and other forecast models.
- 12 • Forecast lead time impacts the accuracy of wave height and storm surge predictions.



13 **Abstract**

14

15 An automated real-time forecast model of surface hydrodynamics in Lake Ontario (Coastlines-LO) was
16 developed to predict storm surge and surface waves. The system uses a dynamically coupled Delft3D –
17 SWAN model with a structured grid to generate 48 h predictions for the lake that are updated every 6 h.
18 The lake surface is forced with meteorological data from the High Resolution Deterministic Prediction
19 System (HRDPS). The forecast model has been running since May 2021, capturing a wide variety of storm
20 conditions. Good agreement between observations and modelled results is achieved, with root mean squared
21 errors (RMSE) for water levels and waves under 0.02 m and 0.26 m, respectively. During storm events, the
22 magnitude and timing of storm surges are accurately predicted at 9 monitoring stations (RMSE < 0.05 m),
23 with model accuracy either improving or remaining consistent with decreasing forecast length. Forecast
24 significant wave heights agree with observed data (1-12% relative error for peak wave heights) at 4 wave
25 buoys in the lake. Coastlines-LO forecasts for storm surge prediction for two consecutive storm events were
26 compared to those from the Great Lakes Coastal Forecasting System (GLCFS) to further evaluate model
27 performance. Both systems achieved comparable results with average RMSEs of 0.02 m. Coastlines-LO is
28 an open-source wrapper code driven by open-data and has a relatively low computational demand,
29 compared to GLCFS, making this approach suitable for forecasting marine conditions in other coastal
30 regions.

31

32 **1 Introduction**

33

34 Coastal regions of large lakes can face hazardous conditions with costly consequences due to strong storm
35 events, where powerful winds generate large waves and storm surge (Danard, 2003; FEMA, 2014;
36 Gallagher et al., 2020). Waves during these events can cause erosion, overtopping, and run-up, with the
37 hazards being greater when the water level is elevated from storm surge. The intensity and frequency of
38 strong storm events is increasing in the Great Lakes region as a result of climate change, as tropical storms
39 are predicted to reach higher latitudes more often (Bender et al., 2010; Studholme et al., 2022). In addition,
40 the mean water levels in the Great Lakes are being impacted by climate change, with large seasonal
41 fluctuations in lake levels and record low and high water levels consistently occurring in recent years
42 (Gronewold and Rood, 2019). The combined impacts of these projections present a greater risk for
43 hazardous conditions in Great Lakes coastal regions, and developing better methods to understand and
44 model the physical processes occurring during storms is important to help mitigate the risk. (Chisholm et
45 al., 2021; Gronewold et al., 2013).



46

47 ‘Real-time forecasting’ of lakes and coastal oceans can be achieved by applying numerical models to run
48 predictive simulations of future hydrodynamic conditions in real time. Water level, circulation, and
49 temperature simulations, using forecast models of large lakes and reservoirs, aid in water quality
50 management (Baracchini et al., 2020; Carey et al., 2021; Lin et al., 2022). Coastal hazard forecasting is also
51 being applied in numerous ocean regions, including the northern Gulf of Mexico where forecast systems of
52 water levels and waves predict hurricane impacts on various scales (Bilskie et al., 2022; Dietrich et al.,
53 2018; Paramygin et al., 2017). Similarly, Rey and Mulligan (2021) use a coupled Delft3D–SWAN model
54 to forecast storm conditions in coastal North Carolina, investigating the influence of various atmospheric
55 forecast models on the results during hurricanes. Specific to lakes, the National Oceanic and Atmospheric
56 Administration (NOAA) has implemented forecast models for North American coastal regions, including
57 the Great Lakes, with the Great Lakes Coastal Forecast System (GLCFS). The GLCFS uses a high-
58 resolution (30 m – 2 km) hydrodynamic model (FVCOM) to simulate physical processes including currents,
59 temperatures, and water levels (Kelley et al., 2018; Peng et al., 2019). Waves in the Great Lakes are
60 predicted by Environment and Climate Change Canada’s (ECCC) Regional Ensemble Wave Prediction
61 System (REWPS), which uses a probabilistic approach to forecast wave characteristic 3 days into the
62 future.

63

64 Developing deterministic forecast models that run in real-time requires dealing with the challenge of
65 minimizing the computational runtime of the model while still achieving accurate results (model resolution
66 and performance), as the forecasts must be available in advance of the actual event. In addition, clear and
67 efficient dissemination of forecasts must be provided to users and stakeholders. Typical real-time coastal
68 models require large computing resources to run high resolution and accurate forecast simulations (Bilskie
69 et al., 2022; Kelley et al., 2018), while fewer model applications focus on developing flexible systems that
70 can achieve accurate results while running on local computers, often for smaller domains, using open data
71 and with a smaller computational allowance (Lin et al., 2022; Rey and Mulligan, 2021).

72

73 The accuracy of numerical models for simulating the hydrodynamic response of coastal regions to storm
74 events has increased with advances in computing power, data availability, and the development of models
75 that can better represent more physical processes and their interactions, however model performance is still
76 limited by the quality of input and forcing data available for a simulation. Model ability also depends on
77 the grid resolution, with higher resolution models being more capable of resolving bathymetric features
78 (Bilskie et al., 2022), and the inclusion of relevant processes, such as wave-current interactions and
79 baroclinic effects (Asher et al., 2019; Swatridge et al., 2022). A main consideration is the accuracy of the



80 atmospheric forcing, as winds are the primary driver of surface behaviour, and errors in the winds translate
81 through as errors in the modelled results (Dietrich et al., 2018; Farhadzadeh and Gangai, 2017; Rey and
82 Mulligan, 2021).

83

84 A probabilistic approach can be used to account for uncertainty in atmospheric forcing by running multiple
85 variations of the same event, however this requires large computational resources (Baracchini et al., 2020;
86 Fleming et al., 2008). In deterministic forecasts of water levels in Lake Erie, error in the atmospheric forcing
87 was significantly larger for 240 h forecasts compared to the 120 h forecasts, which translated to increased
88 error in predicted water levels (Lin et al., 2022). The longer forecast predicted excessive seiching and an
89 underestimation in peak water level, which improved as forecast length decreased. Forecasts of hurricane
90 storm surge and waves in the Gulf of Mexico by Forbes et al. (2010), Dietrich et al. (2018), and Bilskie et
91 al. (2022) found trends of decreasing error in storm surge prediction with shorter forecast length. Longer
92 forecasts (~5 days) resulted in storm surge variations of up to 4 m from the best track predictions, attributed
93 to variability in atmospheric forcing, and for forecasts shorter than 2.5 days, simulations converged on a
94 solution, and error was almost constant (Dietrich et al., 2018).

95

96 The hydrodynamics of Lake Ontario have been simulated on various scales in previous studies (e.g., Huang
97 et al., 2010; Paturi et al., 2012; Prakesh et al., 2007; Shore, 2009). Numerical models have also been used
98 to simulate waves and circulation during extreme events in the Kingston Basin (Cooper and Mulligan, 2016;
99 McCombs et al., 2014a; McCombs et al., 2014b). Sogut et al. (2019) used a combination of analyzing
100 historical water level and wave data, as well as numerical modelling of extreme storm events to gain insight
101 on lake seiching, storm surges, and wave patterns. Historical data have also been studied to determine the
102 risk of flooding due to storm surge along the Lake Ontario shoreline with a statistical model (Steinschneider,
103 2021). Surface waves and storm surge were simulated over the entire lake by Swatridge et al. (2022) during
104 recent storm events. Their study investigated the influence of different wind fields on the accuracy of storm
105 surge simulation, finding that variations in meteorological forcing were the primary source of uncertainty
106 in model results.

107

108 In the present study, an existing depth-averaged numerical model of Lake Ontario (Swatridge et al., 2022)
109 was applied to the lake to forecast water levels and waves in real-time, driven by spatially varied wind
110 fields from a high-resolution wind forecast model. The workflow develops an open-source Python- and
111 MATLAB-based wrapper code, that has been successfully applied to other systems using different
112 hydrodynamic models as part of the Canadian Coastal and Lake Forecasting Model System (Coastlines;
113 <https://coastlines.engineering.queensu.ca>; Lin et al., 2022; Rey and Mulligan, 2021). This flexible



114 methodology uses open access forcing/validation data and requires a relatively low computational demand,
115 compared to other existing Great Lakes storm surge models, allowing for application to other locations.
116 Model performance is evaluated by comparing results to near-real time observed data. Forecast results, for
117 storm surges and waves are statistically investigated over forecast lead times ranging from 6 to 48 h.

118

119 **2 Methods**

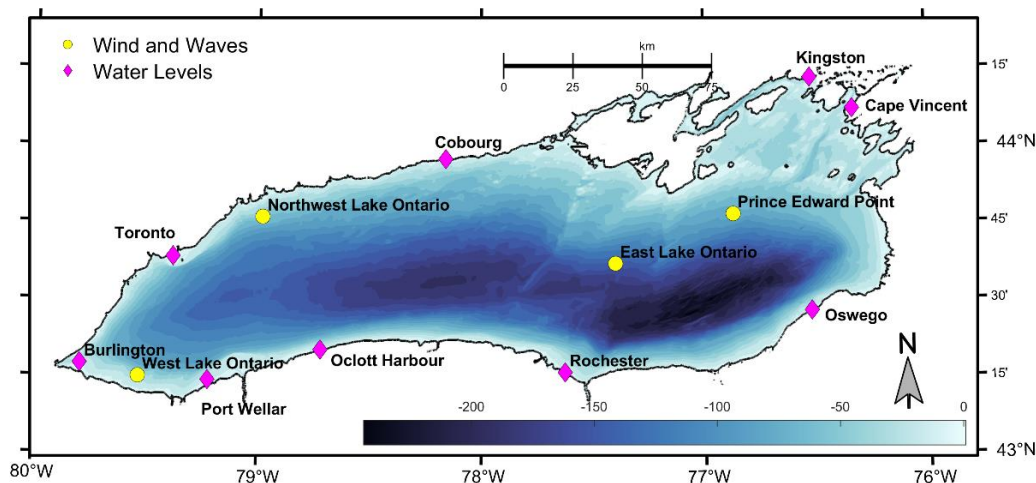
120

121 *2.1. Modelling Approach*

122 A two-dimensional (depth-averaged) coupled hydrodynamic-wave model is applied to Lake Ontario to
123 simulate wind driven hydrodynamics and waves using Delft3D-SWAN. The Delft3D flow model calculates
124 non-steady flow on a structured grid by solving the Reynolds-Averaged Navier Stokes equations (Lesser et
125 al., 2004). Wave conditions are simulated with the phase-averaged wave model, Simulating Waves
126 Nearshore (SWAN), which uses the spectral action balance equation to compute random wind-generated
127 waves. SWAN accounts for non-linear wave interactions, wave propagation, refraction, dissipation due to
128 whitecapping, bottom friction and depth-induced breaking (Booij et al., 1999). The models are dynamically
129 coupled to account for wave-current interactions. Radiation stress gradients from SWAN simulations are
130 input into the horizontal momentum equations in Delft3D to account for the impacts of waves on
131 circulation, such as wave-induced mass fluxes driving currents, and enhanced bed shear stress. Results from
132 the hydrodynamic simulation are then used to update water levels and circulation in the wave model.

133

134 Model setup choices were made based on simulations by Swatridge et al. (2022) which were adapted for
135 the present study to minimize computational demand, allowing the system to run in real-time. The Delft3D
136 simulation uses a curvilinear grid with a horizontal resolution gradually ranging from 250-450 m, with
137 higher resolution in nearshore areas, and a coarser grid with resolution ranging from 350-600 m for the
138 wave model. Flow simulations are depth-averaged and barotropic, shown by Swatridge et al. (2022) to
139 accurately represent surface storm surge in Lake Ontario, with root mean squared errors (RMSEs) between
140 observations and model results ranging between 0.01 m - 0.07m during several major events. Bathymetry
141 data was interpolated to the grid from the US National Centers for Environmental Information's (NCEI) 3-
142 arcsecond (~ 90 m) resolution dataset with supplementary data from the ETOPO1 global relief model with
143 a resolution of approximately 1.3 km (Fig. 1). Detailed sensitivity testing for this model was completed in
144 Swatridge et al. (2022) to calibrate model parameters. Simulations use a time step of 120 s to satisfy the
145 Courant–Friedrichs–Lewy stability criterion and coupling between the flow and wave models occurs every
146 60 minutes.



147

148 **Figure 1:** Map of Lake Ontario showing bathymetry and the location of real-time water level, wind, and
149 wave observation stations.

150

151 Spatially varied atmospheric input from the Meteorological Service of Canada (MSC) High Resolution
152 Deterministic Prediction System (HRDPS) is used to drive the model (Milbrandt et al., 2016). HRDPS is
153 an hourly assimilated forecast system downscaled from the larger scale Regional Deterministic Prediction
154 System (RDPS) that provides hourly predictions of surface pressure and wind velocity components with a
155 horizontal resolution of 2.5 km for the pan-Canada domain. The system runs every 6 h, predicting
156 atmospheric conditions 48 h into the future. This wind-forcing was successfully used by Swatridge et al.
157 (2022) to simulate the lake surface response to a range of storm conditions. Their modelled results for water
158 levels and surface waves agreed with observations at up to 16 locations in Lake Ontario, resulting in
159 maximum difference between predicted and observed peak wave heights and water levels of 0.4 m and
160 0.08 m, respectively. No lateral open boundary conditions are applied to account for inflows and outflows
161 to the lake, as previous work has found the major riverine flows (Niagara and St. Lawrence Rivers) have a
162 negligible hydrodynamic influence on large-scale circulation and water levels over event-based timescales
163 (Prakash et al., 2007).

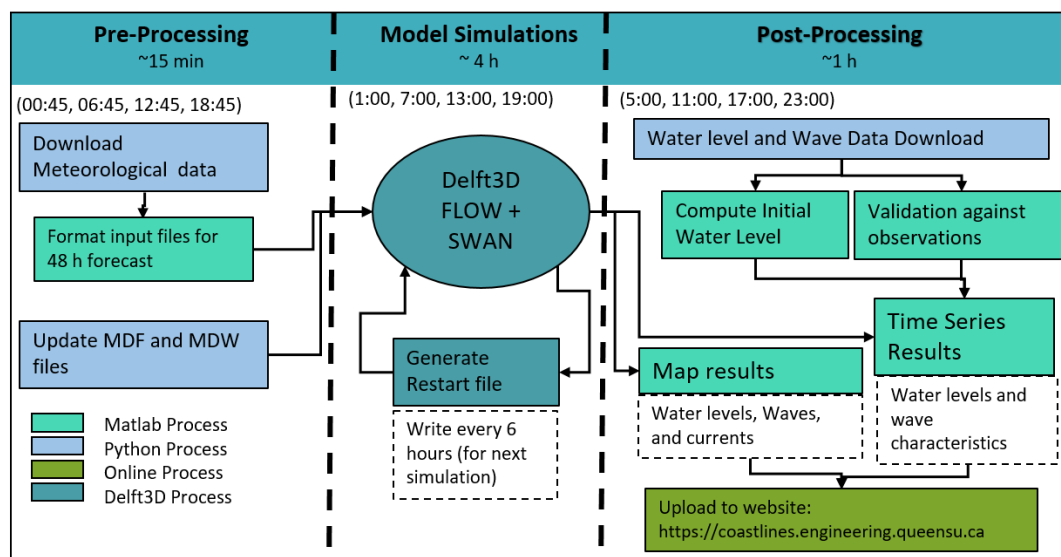
164

165 2.2. Development of an Automated Prediction System

166 The forecast system uses a combination of code written in MATLAB and Python to automatically run every
167 6 h and has been operational since May 2021 (<https://coastlines.engineering.queensu.ca/lake-ontario/>). The
168 workflow (Fig 2) consists of pre-processing, model simulation and post processing stages. For pre-



169 processing, the system is initiated when a new HRDPS forecast becomes available. Python is used to
170 download the latest forecast and MATLAB is used to automatically process the atmospheric forcing and
171 write input files for Delft3D-SWAN. The Delft3D model definition files are then updated with the correct
172 time information.



173
174 **Figure 2.** Diagram of the automated workflow for processes performed for each model cycle (every 6 h
175 initiated by Windows Task Scheduler) on the local Coastlines server.

176
177 Model simulations cover a period of 48 h and are ‘hot-started’ with a restart file from a previous model run
178 if available. If a restart file is not available, simulations begin from rest with initial water levels of 0 m and
179 current speeds (u) of 0 m s^{-1} throughout the lake. When the simulation finishes, all available real-time
180 observed data, outlined in Table S1 in the supplementary material, is downloaded using Python, which is
181 then processed in MATLAB. Observed water levels, at each station, are averaged over the previous 12 h
182 and used to locally adjust the datum of the model outputs. We acknowledge that assimilating observed
183 water levels into the initial conditions may be a preferred approach, but this is beyond the scope of the
184 present study and may be incorporated into future versions on Coastlines-LO. The model simulates high
185 frequency variability in water levels generated by winds. Seasonal changes in water levels due to inflows,
186 outflows, and evaporation are not included, but are accounted for in post-processing.

187
188 Time series plots of observed water levels and wave heights are automatically compared to the forecast
189 model results from the previous 2.5 days at the observation locations and additional plots are created to
190 provide predictions at other locations of interest with no observed data (Fig. 1). Spatial snapshots of model



191 results across the lake are generated at select times, as well as animations showing key output parameters
192 during the forecast simulation. All outputs are exported to Google Sheets and displayed on the project
193 webpage, <https://coastlines.engineering.queensu.ca/>. The system runs in a Windows environment using 16
194 cores of a 32-core XEON workstation, with each workflow cycle taking approximately 5 h to complete a
195 48 h forecast simulation.

196

197 *2.3. Real-time Comparison between Model Results and Observations*

198 Near real-time observations of water surface elevation (η) data are available at 9 water level gauges in Lake
199 Ontario from the National Oceanic and Atmospheric Administration (NOAA) and the Department of
200 Fisheries and Oceans Canada (DFO), with temporal resolutions of 3 minutes and 6 minutes, respectively
201 (Fig. 1; Table 1). Hourly surface waves and winds are measured in Lake Ontario at one US National Data
202 Buoy Center (NDBC) buoy and ECCC buoys from spring to early winter (these buoys are removed in
203 winter due to the possibility of ice damage). The buoys report the significant wave height (H_s), peak wave
204 period (T_p), surface wind speed and direction averaged over an 8-minute period (U).

205



206 **Table 1:** List of real-time observed data sources in Lake Ontario

| Name | Longitude | Latitude | Depth | Parameter | Source |
|------------------------|-----------|----------|-------|-------------|--------|
| Prince Edward Point | -76.87 | 43.78 | 68 m | Wave; Wind | ECCC |
| West Lake Ontario | -79.53 | 43.25 | 35 m | Wave; Wind | NDBC |
| Northwest Lake Ontario | -78.98 | 43.77 | 54 m | Wave; Wind | NDBC |
| East Lake Ontario | -77.40 | 43.62 | 140 m | Wave; Wind | NDBC |
| Oswego | -76.52 | 43.46 | N/A | Water Level | NOAA |
| Rochester | -77.63 | 43.27 | N/A | Water Level | NOAA |
| Olcott Harbour | -78.72 | 43.34 | N/A | Water Level | NOAA |
| Cape Vincent | -76.33 | 44.12 | N/A | Water Level | NOAA |
| Port Wellar | -79.22 | 43.24 | N/A | Water Level | DFO |
| Cobourg | -78.16 | 43.96 | N/A | Water Level | DFO |
| Burlington | -79.79 | 43.29 | N/A | Water Level | DFO |
| Kingston | -76.52 | 44.22 | N/A | Water Level | DFO |
| Toronto | -79.38 | 43.64 | N/A | Water Level | DFO |

207

208 For long term analysis of results, the residual component of the water level data, representing storm surge,
209 is isolated at the gauge locations by finding the difference between the total water level and the average
210 water level, calculated using a gaussian window of 7 days (Steinschneider et al., 2021). Model performance
211 is quantified by computing error statistics, including the RMSE, normalized RMSE (NRMSE), and the
212 correlation coefficient (r). Strong storm surge events are identified from the water level data using the
213 peaks-over-threshold method (Steinschneider et al. 2021). Forecast error, during select events, was
214 evaluated by computing error metrics for consecutive forecasts leading up to the peak of the event. For each
215 forecast, the relative error (RE), between observed and simulated maximum storm surge or wave heights,
216 was computed, and the RMSE was computed over a 6 h period that included the peak of the event.

217

218 **3 Results**

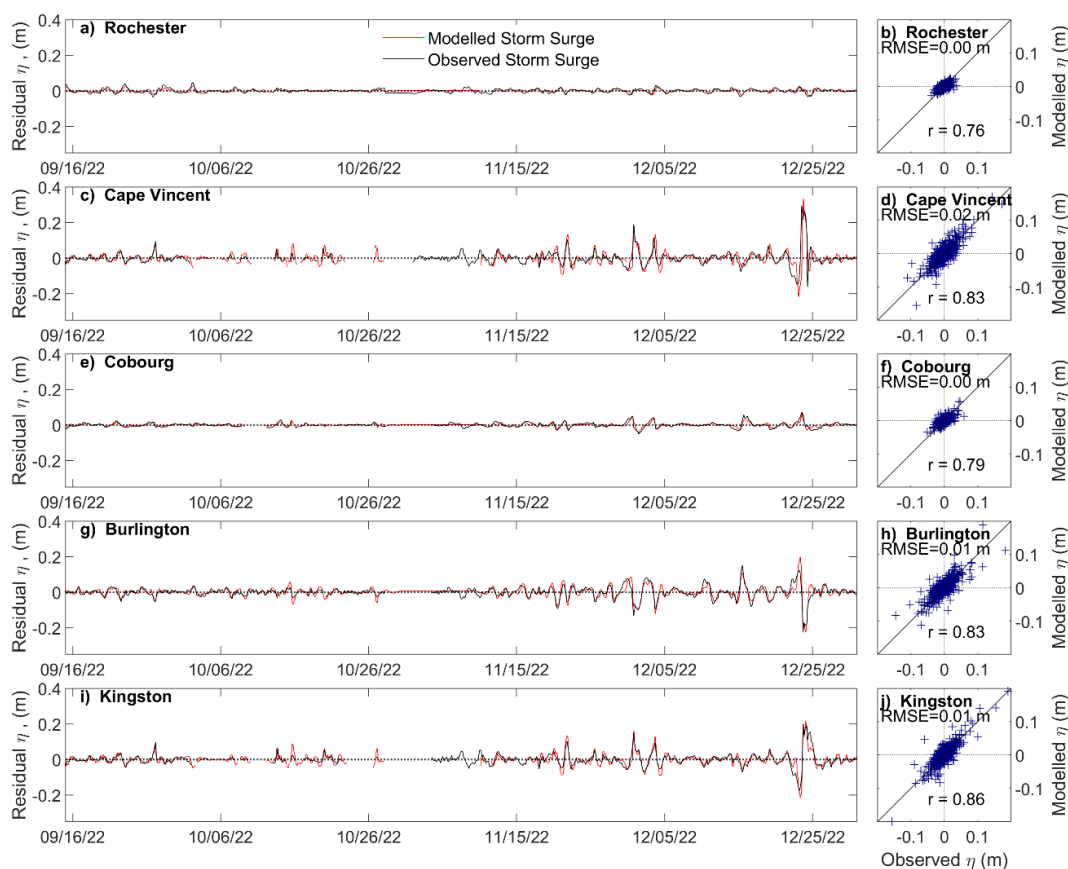
219

220 *3.1. Long-term model performance*

221 Simulation results, for water levels and waves, at the observation locations, were compiled over the 20-
222 month operational period. The first 6 h of each 48 h forecast were stitched into a single time series, and
223 these results were compared to the observed data (Fig. S1 in the supplementary material). During this time,
224 seasonal changes in the observed mean lake level fluctuated by over 1 m, with the highest water levels



225 occurring in May 2022. The ability of the model to reproduce storm surge was investigated over a four-
226 month period when multiple storm events occurred (106 days from 15 September 2022 to 30 December
227 2022; Fig. 3). Stations with larger ranges of observed water levels (i.e., Burlington, Cape Vincent), located
228 at the east and west ends of the lake (i.e., Fig. 3c, g, i) show a slight bias, where the model tended to slightly
229 overpredict maximum and minimum values, corresponding to larger RMSE values (Table 2). These stations
230 also tended to show a stronger correlation ($r = 0.83 - 0.86$); whereas observation points with typically
231 smaller ranges in water levels (Fig. 3a, c) resulted in weaker correlations ($r = 0.76 - 0.79$). Normalized
232 results show comparable error statistics at all stations, with larger errors occurring at locations with smaller
233 storm surges (i.e., Rochester, Oswego).
234



235
236 **Figure 3:** Observed (black) and modelled (red) residual water levels at select observation points over a 3
237 month period (September – December 2022) with corresponding scatter plots and error statistics over this
238 period at select locations.
239



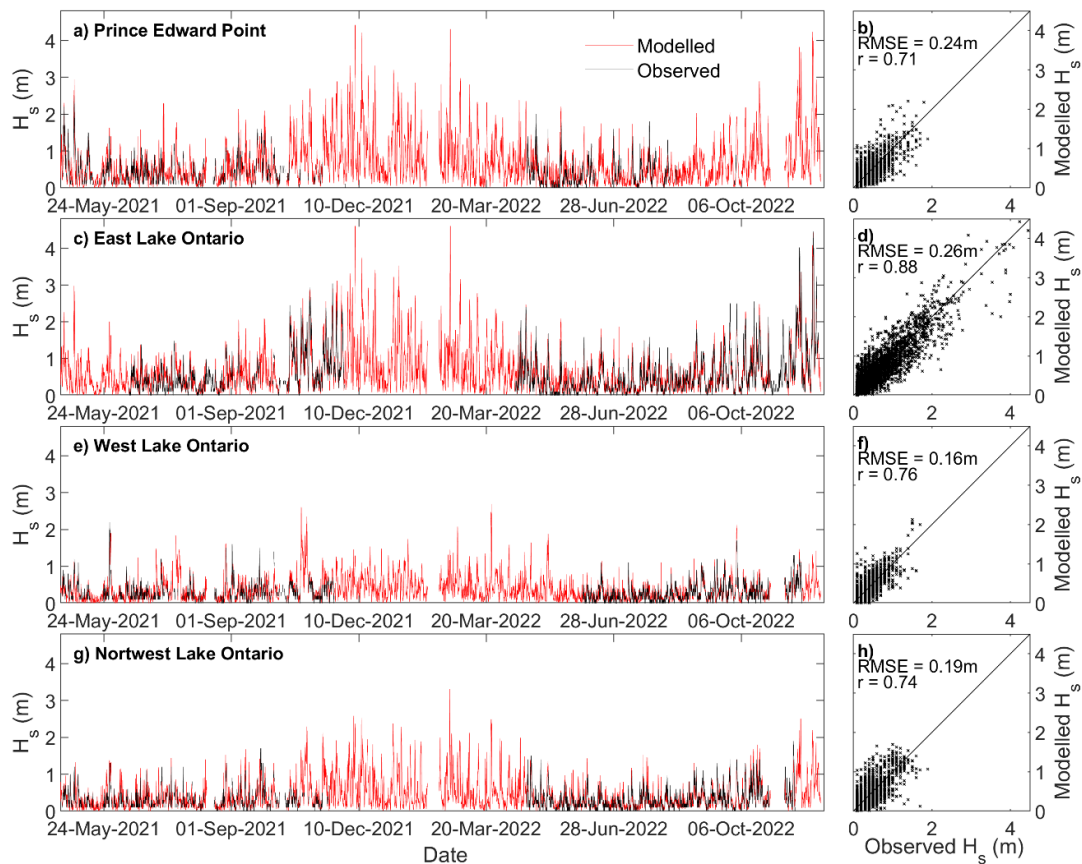
240 **Table 2:** Error Statistics for residual water level results over 106 days (September 15 – December 30, 2022)

| | Minimum η (m) | Mean η (m) | Maximum η (m) | RMSE (m) | NRMSE (m) | r |
|--------------|-----------------------|--------------------|-----------------------|-------------|--------------|------|
| Oswego | -0.10 | 0.07 | 0.12 | 0.01 | 0.15 | 0.80 |
| Rochester | -0.03 | 0.03 | 0.04 | 0.00 | 0.16 | 0.76 |
| Olcott | -0.16 | 0.04 | 0.11 | 0.01 | 0.19 | 0.80 |
| Cape Vincent | -0.22 | 0.10 | 0.34 | 0.02 | 0.16 | 0.83 |
| Port Wellar | -0.19 | 0.06 | 0.16 | 0.01 | 0.14 | 0.86 |
| Cobourg | -0.08 | 0.04 | 0.07 | 0.01 | 0.14 | 0.79 |
| Toronto | -0.16 | 0.07 | 0.14 | 0.01 | 0.14 | 0.83 |
| Burlington | -0.22 | 0.10 | 0.20 | 0.02 | 0.14 | 0.83 |
| Kingston | -0.21 | 0.09 | 0.25 | 0.01 | 0.14 | 0.86 |

241

242 Results for simulated H_s over the 600-day operational period at buoy locations show the largest waves
 243 occurred during winter, between December and March (Fig.4). During this time, no monitoring data was
 244 available for comparison and Lake Ontario could potentially experience partial ice-cover in nearshore areas,
 245 impacting the wave environment (Anderson et al., 2018). Stations in the northeast region of the lake (Prince
 246 Edward Point, East Lake Ontario) generally experienced the largest waves, due to the prominent north-
 247 easterly direction of storms over the lake resulting in a larger fetch at these locations. Error statistics show
 248 similar values for RMSE at these points however Prince Edward Point had the lowest correlation coefficient
 249 (Fig. 4a, b; $r = 0.71$), while East Lake Ontario showed the highest correlation (Fig. 4c, d; $r = 0.88$). Lower
 250 RMSE were at stations with smaller waves (Fig. 4e, g), and normalized results (Table 3) show comparable
 251 results at all buoys (NRMSE = 0.42 – 0.53 m).

252



253

254 **Figure 4:** Time series of observed (black) and modelled (red) significant wave height over the duration that
255 the buoys were in the lake (September -December 2022) with corresponding error scatter plots at the
256 location of the 4 buoys.

257



258 **Table 3:** Error statistics for significant wave heights at the buoy locations over 600 days (April 21, 2021 –
259 December 12, 2022)

| Location | Mean H_s (m) | Maximum H_s (m) | RMSE (m) | r | NRMSE (m) |
|------------------------|----------------|-------------------|----------|------|-----------|
| Prince Edward Point | 0.44 | 3.82 | 0.24 | 0.71 | 0.53 |
| East Lake Ontario | 0.62 | 4.42 | 0.26 | 0.88 | 0.42 |
| West Lake Ontario | 0.34 | 2.60 | 0.16 | 0.76 | 0.48 |
| Northwest Lake Ontario | 0.35 | 2.29 | 0.19 | 0.74 | 0.53 |

260

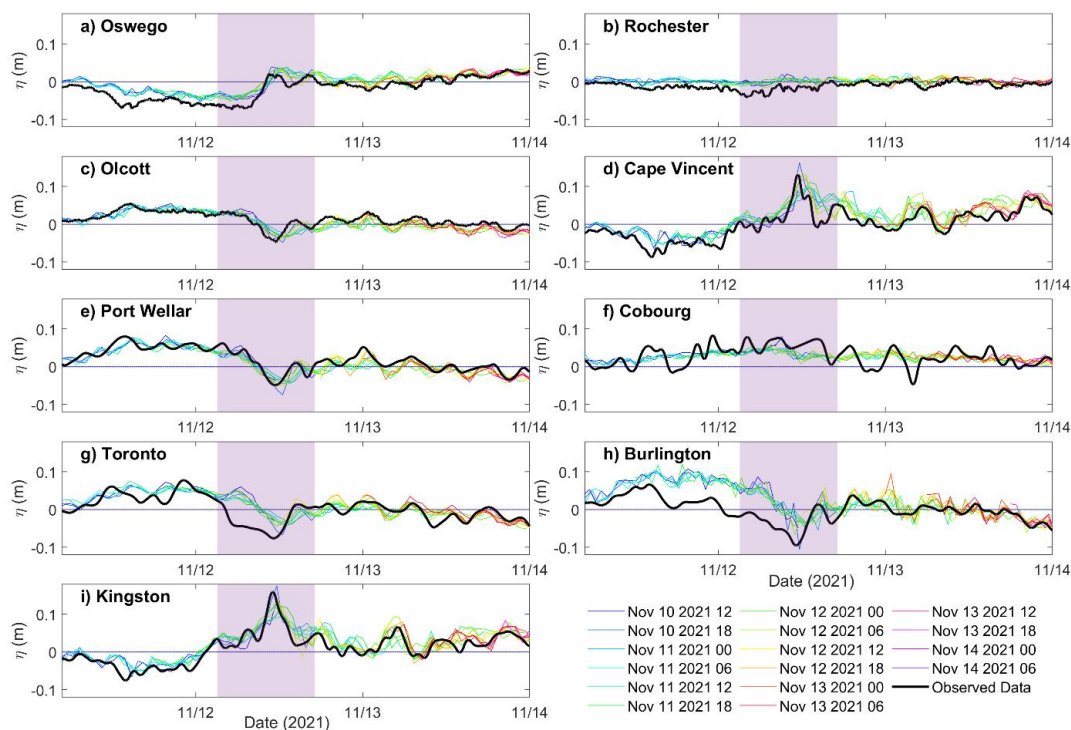
261 *3.2. Storm event forecasts*

262 The performance of the model was evaluated during an event on November 11, 2021. During this event,
263 wind speeds reached up to 15 m s^{-1} , with the direction rotating clockwise from the southeast to the west
264 over a 24 h period. Overlapping 48 h HRDPS forecasts (i.e., generated every 6 h) were validated against
265 buoy observations, with good agreement found between modelled and predicted total wind speeds and
266 directions, with peak wind speeds underrepresented by at most, 4.21 m s^{-1} at Northwest Lake Ontario and
267 overpredicted by up to 2.61 m s^{-1} at Prince Edward Point (Fig. S2 in the supplementary material)

268

269 This event resulted in an observed storm surge of up to 0.16 m in the northeast region of the lake, at Cape
270 Vincent and Kingston. The forecast simulations captured the timing and magnitude of the event peak, with
271 predicted surge values ranging between 0.12 m – 0.17 m (Fig.5d, i). A set down of about 0.10 m was
272 recorded at the Burlington station, which was underpredicted by the model by up to 0.05 m. The simulated
273 results at this location predicted water levels up to 0.05 m higher than the observations for the 24 h preceding
274 the storm (Fig.5h). Notable error can also be identified at Cobourg (Fig. 5f) with the model predicting
275 negligible fluctuations in the water surface, but observations show some oscillations (0.05 m).

276



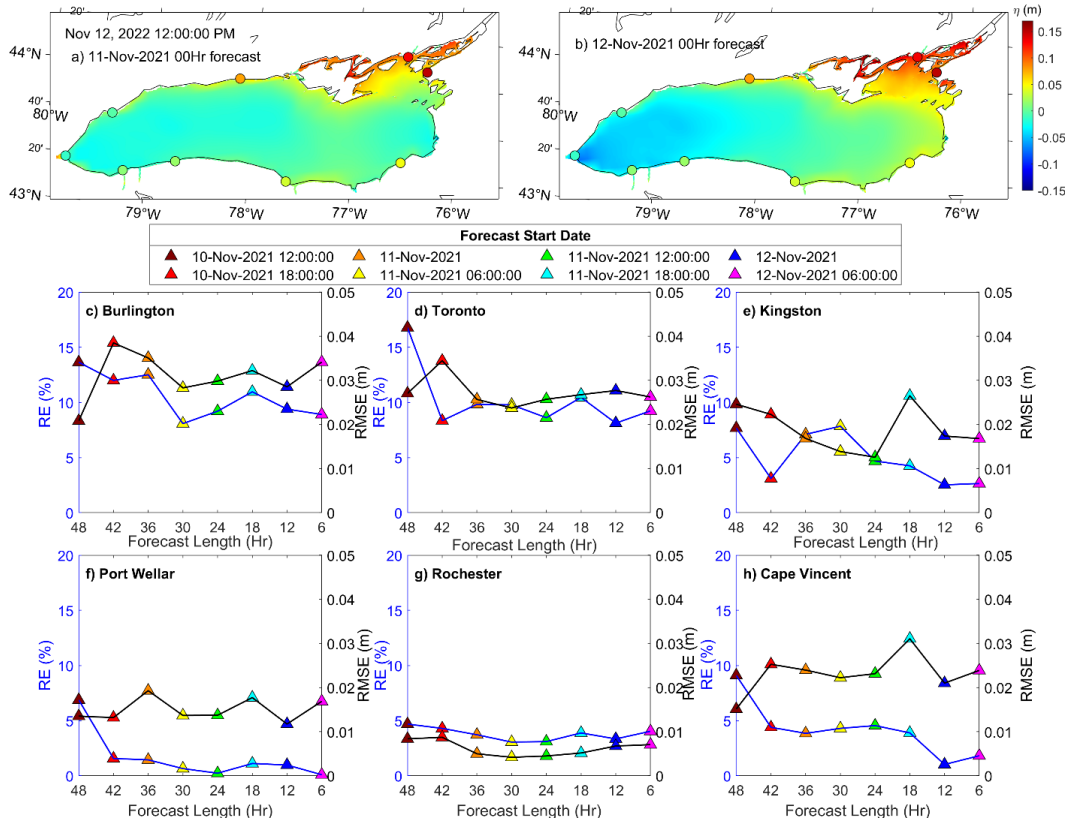
277

278 **Figure 5:** Time series of measured water levels at various observation points compared to forecasted data
279 from progressive model simulations. The highlighted area indicates the time over which error statistics are
280 computed.

281

282 Forecast performance was quantified by computing error statistics, over the duration of the event, for each
283 forecast leading up to the time of peak water level. The largest errors occurred at the location of the set
284 down, Burlington and Toronto, with a nearly constant RMSE of 0.03 m, and RE of 12% and 10%
285 respectively (Fig. 6c, d). The errors at all stations remained fairly constant with RMSE and RE under 0.03 m
286 and 10%, respectively, for each new forecast. However, map results showing the spatial variability in water
287 level predictions from forecasts 12 h and 36 h before the storm peak show large differences (Fig. 6a,b). The
288 earlier results (Fig. 6a) simulated a far less extensive storm surge in the northeast region of the lake than
289 what was subsequently predicted 24 h later (Fig. 6b), when the storm surge was simulated to impact most
290 of the northeast shoreline. The later forecast also predicted spatially larger set-down, about 0.10 m more
291 than the earlier forecast in the western region of the lake.

292



293

294

295

296

297

298

299

300

301

302

303

304

305

306

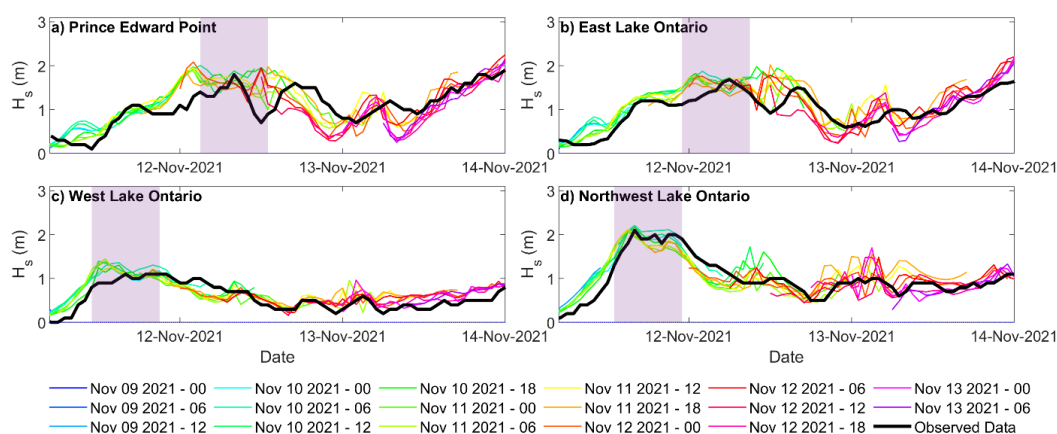
307

Figure 6: Contour plots showing maps of modelled water levels at the peak of the storm event from two different forecasts, starting a) November 11, 00:00 UTC and b) November 12, 00:00 UTC with observed data plotted at the observation locations in black circles. Panels c) to h) show metrics including the Relative Error (RE) and Root Mean Square Error (RMSE) for peak storm surge magnitude at the locations of 6 selected water level gauges from the 8 forecasts preceding the storm event.

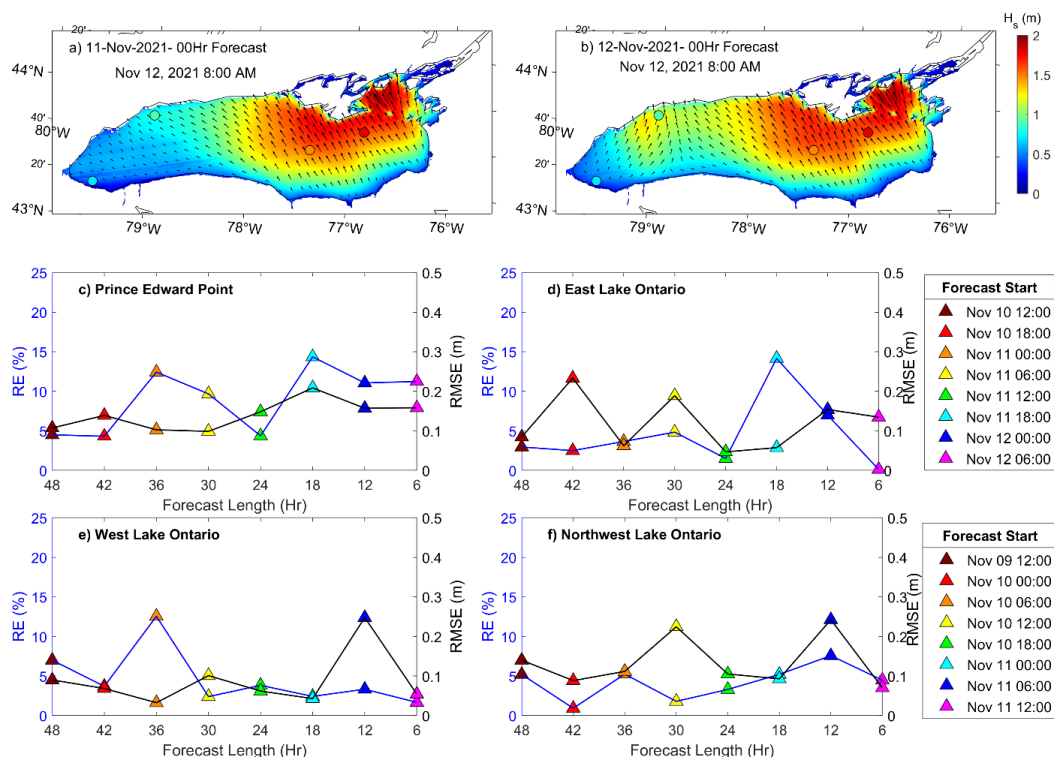
Measured waves during this event reached up to 2.10 m, with the buoys in the western region of the lake (Fig. 7c, d) experiencing peak wave heights about 12 h earlier than the buoys in the eastern region of the lake (Fig. 7a, b), due to the shift in wind direction during the storm. Overall, forecast simulations captured the magnitude of the waves all stations, with some error, and approximately 5 h delay in the timing of the peak H_s at Prince Edward Point (Fig. 7a). Error for waves during this event, at all stations, was constant for consecutive forecasts at all stations, with RMSE between 0.03 – 0.25 m and RE between 1-12%. Despite the generally consistent results, at the buoy locations, maps from different forecasts show distinct changes between the 36 h forecast (Fig. 8a) and the 6 h forecast (Fig. 8b). Simulated wave fields in the northeast



308 region of the lake showed similar results between forecasts, but in the northwest, predicted wave
309 magnitudes and directions were distinctly different. The earlier forecast predicted waves under 0.70 m
310 coming from the southeast, whereas the later forecast showed larger waves ($H_s = 0.50 - 1.00$ m) from the
311 southwest, which can be attributed to changes in forecasted wind-fields.
312



313
314 **Figure 7:** Time series of measured H_s at the location of the 4 buoys compared to modelled data from
315 progressive model forecasts for Event 1 (November 12, 2021). The highlighted area indicates the time over
316 which error statistics are computed.



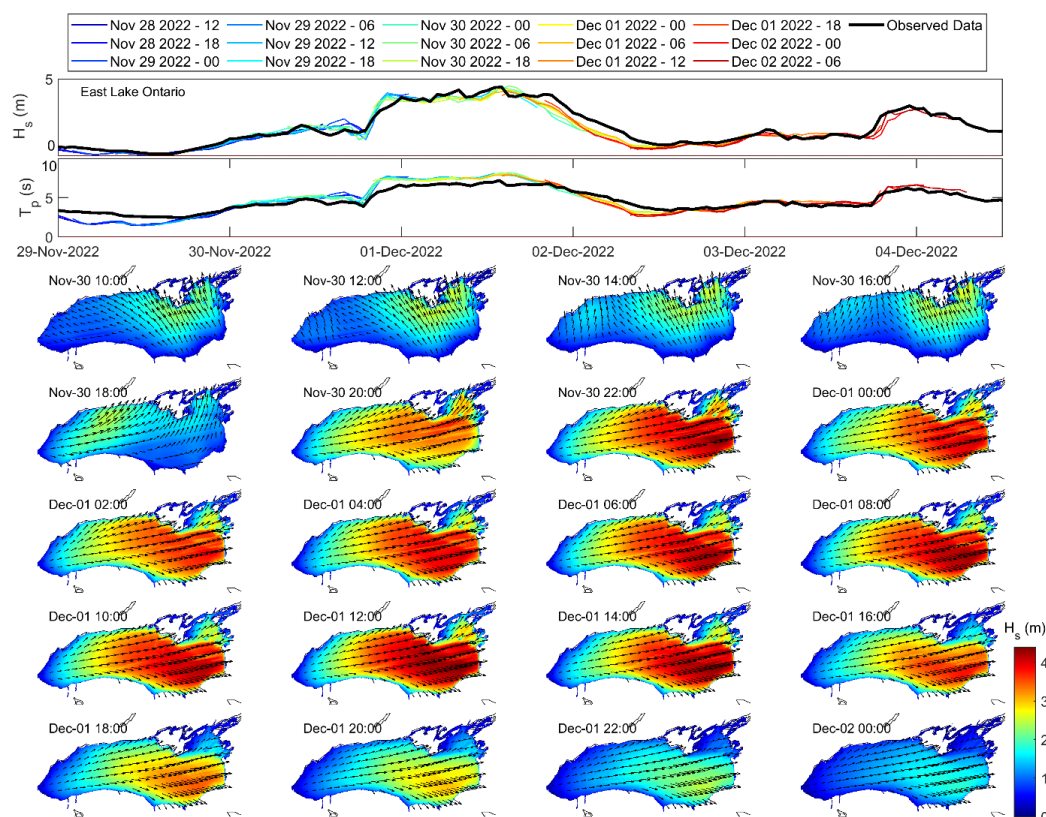
317
 318 **Figure 8:** Contour plots showing maps of modelled waves at the peak of the storm event from two forecasts,
 319 starting a) November 11, 00:00 UTC and b) November 12, 00:00 UTC with observed data plotted at the
 320 observation locations in black circles. Panels c) to f) show metrics including the Relative Error (RE) and
 321 Root Mean Square Error (RMSE) for significant wave height at the locations of 4 buoys from the 8 forecasts
 322 preceding the storm event on November 12, 2021, 12:00 UTC.

323

324 For further investigation into model performance during storm events, wave forecasts during the event that
 325 resulted in the largest observed wave heights (December 1, 2022, Fig. 3c) were examined. During this
 326 storm, the lake experienced sustained easterly winds for almost 24 h, reaching speeds $> 20 \text{ m s}^{-1}$ on
 327 December 1, 14:00 UTC, generating waves $> 4 \text{ m}$ (Fig. 9). Data was only available from the one buoy at
 328 East Lake Ontario during this event, which recorded a maximum $H_s = 4.46 \text{ m}$. The forecasts initially
 329 underestimated this value, with a maximum predicted wave height of $H_s = 4.19 \text{ m}$ from the forecast starting
 330 on November 29 18:00 UTC, and the next forecast then overestimated this value ($H_s = 4.54 \text{ m}$). Subsequent
 331 forecasts slightly underestimated the peak value, with the lowest predicted peak $H_s = 4.26 \text{ m}$ and the
 332 maximum values occurring $\sim 1 \text{ h}$ after the observed peak. All forecast results tended to overestimate the



333 peak wave period, with predicted values ranging between 7.8 - 8.1 s, compared to an observed maximum
334 value of 7.2 s.
335



336
337 **Figure 9:** Variability in significant wave height during a storm event: measured H_s compared to progressive
338 forecast results at the Prince Edward Point Buoy for Event 3 (December 1, 2022; top) and maps of H_s and
339 wave direction shown at an interval of 2 h (every 10th vector is shown for clarity).

341 4 Discussion

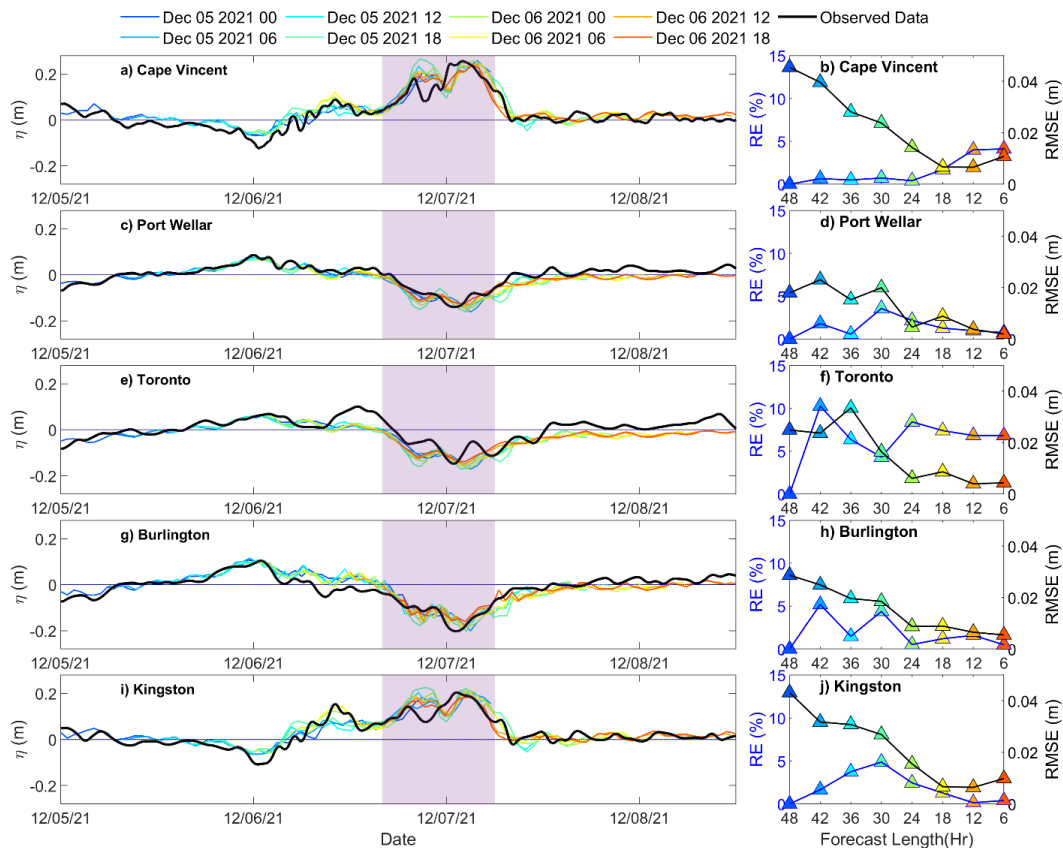
343 4.1. Forecast Lead Times

344 Water level forecasts during a storm event on December 8, 2021, were examined in relation to forecast lead
345 time. During this event, 21 m s⁻¹ winds generated a storm surge of approximately 0.20 m along the northeast
346 coast, and a resulting setdown of 0.10 m on the opposite end of the lake. Error statistics throughout the peak



347 of the event, as a function of forecast lead time, were plotted at select stations (Fig. 10). The timing and
348 magnitude of the storm surge was well represented by the forecast model, with RMSE < 0.05 m for all
349 forecasts and a maximum RE =14%.

350



351

352 **Figure 10:** Time series of measured water levels at select observation points compared to forecasted data
353 from progressive model simulations for Event 3: December 08, 2021, with corresponding plots showing
354 computed RMSE calculated over the shaded area and percent error in peak storm surge from the 8 forecasts
355 preceding the storm event.

356

357 Trends in the error can be identified for this event at all stations, with notable patterns corresponding to
358 locations with larger fluctuations in water level (i.e., Cape Vincent, Kingston, Burlington). At these sites,
359 forecast error tended to decrease as the forecast length shortened. At Cape Vincent, the initial 48 h forecast
360 had an RMSE of 0.05 m and by the 18 h forecast, the RMSE had decreased to 0.01 m. However, after the
361 18 h forecast there was a slight increase in RE from less than 1% to about 5% (Fig. 10b). Trends in



362 decreasing error were also observed at Kingston, where a similar decrease in RMSE was observed, and the
363 RE was maintained between 1 – 5%, corresponding to a maximum underprediction of about 0.05 m (Fig.
364 10i, j). The locations with smaller ranges in surface fluctuations (Toronto, Port Wellar) generally showed
365 constant error (0.02 m and ~1% at Port Wellar; 0.01 m and 7% at Toronto) for consecutive forecast results
366 over the duration of this event (Fig. 10d, f).

367

368 Hydrodynamics in the model are only driven by atmospheric forcing, which is a primary source of
369 uncertainty in simulations of surface dynamics in large lakes. The accuracy of meteorological forecasts
370 typically decreases with increasing length due to assimilation schemes using observations and satellite
371 imagery to yield more accurate results (Buehner et al., 2015). Therefore, it is expected that hydrodynamic
372 forecast simulations will increase in accuracy as the lead time to a storm event decreases. For forecasts of
373 storm surges in other Great Lakes (e.g., Lake Erie; Lin et al., 2022) and coastal seas (e.g., Gulf of Mexico;
374 Dietrich et al., 2018), improvements in storm surge predictions are directly linked to increased accuracy in
375 meteorological forcing leading up to an event. However, our Lake Ontario model results do not follow a
376 consistent trend between different events, either improving (Fig. 10) or maintaining accuracy (Fig. 6;
377 Fig. 8). Despite model accuracy being constant at the observation locations, changes in the spatial
378 variability of predicted water levels and wave conditions for different forecasts are not clearly
379 communicated through time series analysis but are qualitatively shown in maps of results (Fig. 6; Fig. 10).

380

381

382 *4.2. Comparison with Other Models*

383 The current work (Coastlines-LO) makes use of a relatively simple, low computational demand modelling
384 approach. The performance of this model can be compared to the GLCFS, which delivers a higher resolution
385 and more complex forecast system in throughout the Great Lakes. Differences between these models can
386 be explained according to fundamental differences in the setup of each system, including different
387 hydrodynamic models, grid resolutions, and atmospheric forcing inputs. The GLCFS uses the 2 km
388 horizontal resolution High Resolution Rapid Refresh (HRRR) meteorological forcing, which is comparable
389 to HRDPS (2.5 km), however previous studies have found that wind and direction predictions can vary
390 between these models (Rey and Mulligan, 2021; Swatridge et al., 2022). The inclusion of waves in the two
391 systems is also accounted for differently, with a separate model (WaveWatch III) used to simulate waves
392 in the GLCFS, while Coastlines-LO uses a dynamically coupled wave and flow model that accounts for
393 wave-current interactions. The inclusion of wave coupling in simulations of the Great Lakes can impact
394 water level predictions (Mao and Xia, 2017). The GLCFS runs on NOAA's high performance computing
395 system, and the larger computational power allows it to include 3D baroclinic processes while still running

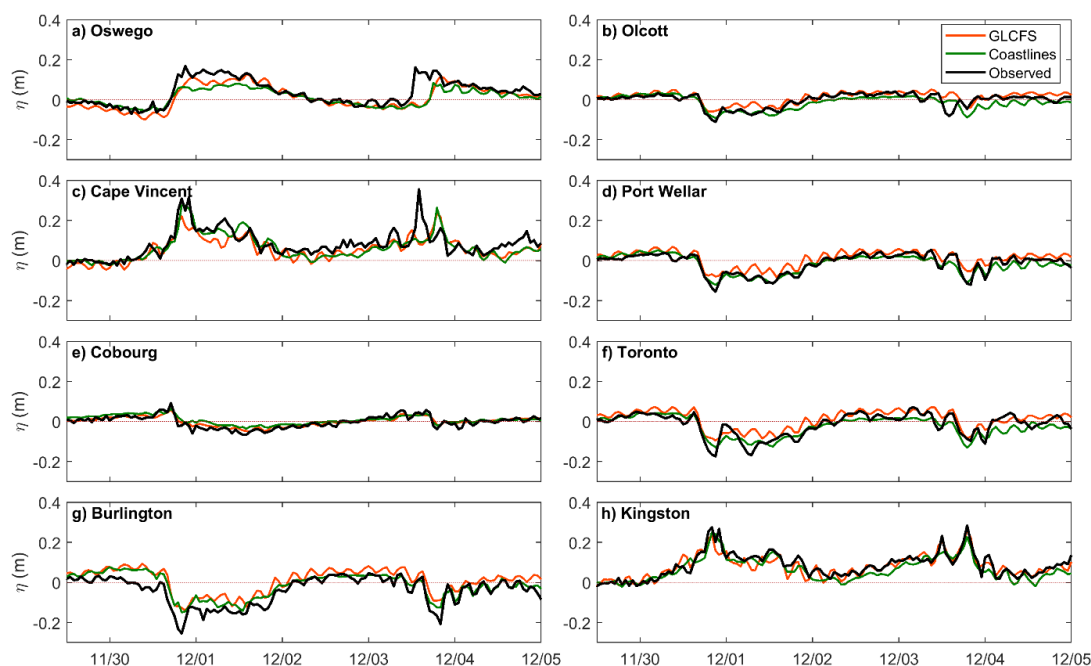


396 in the required timeframe, whereas the Coastlines-LO system in the present study uses a 2D, depth averaged
397 approach, and therefore doesn't resolve vertical gradients in lake temperature or 3D circulation. The
398 inclusion of river inflows and outflows in the GLCFS also allows the model to simulate seasonal changes
399 in the mean lake water level instead of accounting for these changes based on observed data in post-
400 processing.

401

402 Forecasts results from both models were compared to observed data over a 6-day period in December 2022,
403 during which 2 storm events occurred (Fig. 11). Results from the first 6 h of subsequent forecasts are
404 combined to construct a water level time series at observation points for both models for the entire duration.
405 Both models represent trends in water levels over this, resulting in comparable metrics, with an average
406 RMSE 0.02 m for both models, and $r = 0.73$ and 0.74 for Coastlines-LO, and GLCFS, respectively. GLCFS
407 achieved better predictions of peak water levels at Oswego for the event on December 1 ($RE = 30\%$ for
408 GLCFS, $RE = 51\%$ for Coastlines-LO; Fig. 11a), and more accurately represented the surface fluctuations
409 observed over the entire 6 day period at Toronto (Fig. 11f). While GLCFS was able to represent water levels
410 at some locations, Coastlines-LO had higher accuracy predictions at others (Fig. 11c, d). At Port Wellar
411 and Cape Vincent, Coastlines-LO better predicted the peak set-down and set-up on December 1 by 0.01 m
412 and 0.03 m respectively, while GLCFS underpredicted at these locations by 0.05 m and 0.09 m. Both
413 models had difficulty simulating the second storm surge (December 3) at Oswego and Cape Vincent (Fig.
414 11 a, c), where the observed surge occurs approximately 3 h before the predicted peak. At the Kingston
415 station (Fig. 11h), storm surges of 0.25 m and 0.30 m are observed. Coastlines-LO yielded better predictions
416 for the first event, simulating a peak value of 0.24 m, compared to 0.28 m predicted by GLCFS, while
417 GLCFS performed better for the second event, with a predicted storm surges of 0.28 m and 0.22 m for
418 GLCFS and Coastlines-LO, respectively. Therefore, while the GLCFS offers several advantages,
419 Coastlines-LO has the benefit of a low computational demand and usage of the flexible open-source
420 wrapping code and that allows for easy adaption to include different hydrodynamic models and investigate
421 different field sites (e.g., Lin et al., 2022; Rey and Mulligan 2021), while still achieving very comparable
422 results simulating short term water level fluctuations in Lake Ontario.

423



424

425 **Figure 11:** Compiled Coastlines-LO forecast results compared to forecasts from the GLCFS and observed
426 data at select water level gauge locations interpolated to a 30 minute time resolution for 2 subsequent events
427 between November 30 – December 5, 2022.

428

429 4.3. Limitations and Uncertainties

430 Sensitivity testing and calibration of the numerical model this system is based on, comes from the work of
431 Swatridge et al. (2022), which found that 3D simulations of Lake Ontario improved predictions of surface
432 behaviour compared to 2D depth averaged simulations. The 3D simulation allowed the model to account
433 for transfer of surface momentum into baroclinic motions, giving a better representation of current
434 velocities and surface seiching following a storm event, resulting in reduced RMSE during storm events by
435 up to 12%, and improvement in modelled peak storm surge magnitude by up to 0.03 m. While 3D
436 simulations improved accuracy, they also increased the computational runtime of a 24 h simulation from
437 about 2.5 h to 4 h. Ten-day forecasts of 3D hydrodynamic processes in Lake Erie has been achieved by Lin
438 et al. (2022) in using the AEM3D model with a similar Coastlines computational workflow as the current
439 work; however, the Lake Erie model is on a coarser 2 km horizontal grid and does not couple with SWAN
440 to predict surface waves, which is computationally expensive compared to hydrodynamic simulations.
441 Therefore, to apply this model in real-time with a new simulation every 6 h, 2D simulations are used,
442 potentially resulting in up to 12% greater uncertainty in the forecast results.



443

444 There is additional uncertainty in model results during the winter season, when ice forms in the Great Lakes.
445 Lake Ontario typically experiences some ice cover between December and April (Anderson et al., 2018),
446 which impacts lake processes, including water levels, circulation, and waves through limited air-water
447 momentum transfer (Anderson et al., 2018; Farhadzadeh and Gangai, 2017). While ice cover has been
448 simulated in Lake Ontario using other models (e.g., Oveysy et al., 2012), it is presently not available in
449 Delft3D-SWAN. Therefore, simulations of surface behaviour during the ice-covered months would have
450 limited accuracy in ice-covered areas. Future work could incorporate ice cover into the model or apply
451 dynamic masking of ice-covered surfaces using satellite data, to improve results during these months.

452

453 While this system requires low computational resources, making it possible to adapt it for other locations,
454 the applicability of the model is limited by the availability of online data for model forcing and validation.
455 In order account for seasonal changes in mean lake levels, near real-time measurements of water levels are
456 needed in the simulation to adjust the datum in post-processing. However, if no data were available the
457 simulation could include the wind-generated short-term fluctuations in surface levels and real-time
458 operations could continue. The workflow of the model is also limited by the availability of atmospheric
459 forcing data, with any interruptions of service in the HRDPS forecasts causing the hydrodynamic
460 simulations to fail for that run-cycle. Improvements in the system could account for this by providing a
461 secondary source of atmospheric forcing in that case. In future studies, we recommend applying this system
462 to a region in the coastal ocean, therefore requiring the development of real-time forecast inputs of open
463 boundary conditions.

464

465 **5 Conclusions**

466

467 A forecast model for wind-driven hydrodynamics was developed and applied to Lake Ontario using an
468 approach with relatively low computational demand. Wind-waves and water levels were simulated using a
469 dynamically coupled Delft3D-SWAN model driven by high resolution atmospheric forcing. Simulations
470 were able to forecast the wind-driven variability in the lake surface, with seasonal changes in the total water
471 levels accounted for by adjusting the datum for each forecast cycle based on observations of the mean water
472 level. The system provides rapid (~5 h runtime) predictions that are publicly available through the project
473 webpage, with the automated system forecasting a 48 h period every 6 h. The model has been running
474 continuously since April 2021, capturing a variety of storm events with storm surges up to 0.30 m and
475 significant wave heights over 4.00 m. Reliable prediction for wave conditions during winter months are



476 provided by the forecast model when no wave observations are available, however accuracy is limited
477 where ice is present as this process is not included in the modelling system.

478

479 Results show that the model is effective in simulating short term fluctuations in the water levels and wave
480 conditions during strong storm events, with relative errors between observed and forecasted storm surge
481 magnitudes and significant wave heights of less than 15%. Larger errors typically corresponded to locations
482 in the lake with larger ranges in observed water levels. For storm events, as the forecast lead time decreases
483 for progressing forecasts, the simulated results changed as a result of updates to the meteorological forcing.
484 No constant trends in forecast error due to decreasing forecast length were apparent, with forecast accuracy
485 increasing with shorter forecasts in some cases and staying constant at others, but overall results agreed
486 well with observed data for all forecasts leading up to an event, with RMSE for storm surge and waves
487 below 0.05 m and 0.30 m, respectively. The model compared well with other existing forecast models in
488 the Great Lakes (GLCFS), yielding comparable results for water level predictions during multiple storm
489 events. Due to the low computational requirements and pan-Canadian coverage from the High Resolution
490 Deterministic Prediction System forecasts, this model could be adapted to other Canadian lakes and coastal
491 seas with available bathymetry data for storm surge prediction and monitoring.

492

493 **6 Code and Data Availability Statement**

494

495 Real-time model results are available at <https://coastlines.engineering.queensu.ca/lake-ontario/>, and
496 archived on the server, to be made available by contacting the corresponding author. HRDPS input data
497 is available from the Meteorological Service of Canada Datamart and observed data is openly accessible
498 online, as cited in the text. The Python and MATLAB scripts, and data used in this research is archived in
499 the Department of Civil Engineering at Queen's University and will be made available on
500 <https://dataverse.scholarsportal.info/dataverse/queens> upon manuscript acceptance. The open source
501 Delft3D software is available from Deltares (<https://oss.deltares.nl/web/delft3d/>).

502

503 **7 Author contributions**

504

505 The concept of the COASTLINES-LO workflow was designed by RM, LB, SS, and LS, and LS
506 implemented the idea. LS developed the performed the model simulations. All authors contributed to the



507 validation of the model and interpretation of the results. SL wrote the manuscript with contributions from
508 LB, SS, and RM.

509 **8 Acknowledgments**

510

511 Funding for this research was provided by Natural Sciences and Engineering Research Council of Canada
512 (NSERC) under the Discovery Grant program awarded to R.P. Mulligan (RGPIN/04043-2018), and a
513 Queen's Dean's Research Fund award to L. Boegman, R.P. Mulligan and S. Shan.

514

515 **9. References**

516 Anderson, E. J., Fujisaki-Manome, A., Kessler, J., Land, G.A., Chu, P.Y., Kelley, J.G.W., Chen, Y., and
517 Wang, J.: Ice Forecasting in the Next-Generation Great Lakes Operational Forecast System
518 (GLOFS). *J. Mar. Sci. Eng.*, 6(4), 123, <https://doi.org/10.3390/jmse6040123>, 2018.

519 Asher, T.G., Luettich, R.A., Fleming, J.G., and Blandton, B.O.: Low frequency water level correction in
520 storm surge models using data assimilation. *Ocean Modelling*, 144,
521 <https://doi.org/10.1016/j.ocemod.2019.101483>, 2019.

522 Baracchini, T., Wuest, A., and Bouffard, D.: Meteolakes: An operational online three-dimensional
523 forecasting platform for lake hydrodynamics. *Water Research*, 172.1-12,
524 <https://doi.org/10.1016/j.watres.2020.115529>, 2020.

525 Bender, M.A., Knutson, T.R., Tuleya, R.E., Sirutis, J.J., Vecchi, G.A., Garner, S.T. and Held, I.M.:
526 Modeled impact of anthropogenic warming on the frequency of intense Atlantic hurricanes.
527 *Science*, 327(5964), 454-458, DOI: 10.1126/science.1180568, 2010.

528 Bilskie, M.V., Asher, T.G., Miller, P.W., Fleming, J.G., Hagen, S.C. and Luettich Jr. , R.A.: Real-time
529 simulated storm surge predictions during Hurricane Michael (2018), *Wea. Forecasting*, 37, 1085–
530 1102, <https://doi.org/10.1175/WAF-D-21-0132.1>, 2022.

531 Buehner, M., McTaggart-Cowan, R., Beaulne, A., Charette, C., Garand, L., Heilliette, S., et al.:
532 Implementation of Deterministic Weather Forecasting Systems Based on Ensemble-Variational
533 Data-Assimilation at Environment Canada. Part 1: The Global System, *Mon. Wea. Rev.*, 143,
534 2532–2559, <https://doi.org/10.1175/MWR-D-14-00354.1>, 2015.

535 Booij, N., Ris, R.C., and Holthuijsen, L.H.: A third-generation wave model for coastal regions: 1. Model
536 Description and validation. *Journal of Geophysical Research: Oceans*, 104(C4), 7649-7666,
537 <https://doi.org/10.1029/98JC02622>, 1999.

538 Carey, C.C., Woelmer, W.M., Lofton, M.E., Figueiredo, R.J., Bookout, B.J., Corrigan, R.S., et al.:
539 Advancing lake and reservoir water quality management with near-term iterative ecological



- 540 forecasting, *Inland Waters*, 12(1), 107-120, <https://doi.org/10.1080/20442041.2020.1816421>,
541 2022.
- 542 Chisholm, L., Talbot, T., Appleby, W., Tam, B., and Rong, R.: Projected change to air temperature, sea-
543 level rise, and storms for the Gulf of Main region in 2050, *Elem Sci Anth*. 9(1), 1-14,
544 <https://doi.org/10.1525/elementa.2021.00059>, 2021.
- 545 Cooper, A.H., and Mulligan, R.P.: Application of a Spectral Wave Model to assess Breakwater
546 Configurations at a small craft harbour on Lake Ontario, *J. Mar. Sci. Eng.*, 2016, 4(3), 46,
547 <https://doi.org/10.3390/jmse4030046>, 2016,
- 548 Danard, M., Munro, A., and Murty, T.: Storm surge hazard in Canada. *Natural Hazards*, 28, 407–434,
549 <https://doi.org/10.1023/A:1022990310410>, 2003.
- 550 Dietrich, J. C., Muhammad, M., Curcic, M., Fathi, A., Dawson, C. N., Chen, S. S., and Luettich Jr., A.:
551 Sensitivity of Storm Surge Prediction to Atmospheric Forcing during Hurricane Isaac, *J. Waterway*,
552 *Port, Coastal, and Ocean Eng*, 144(1), [https://doi.org/10.1061/\(ASCE\)WW.1943-5460.0000419](https://doi.org/10.1061/(ASCE)WW.1943-5460.0000419),
553 2018.
- 554 Farhadzadeh, A., and Gangai, J.: Numerical Modelling of Coastal Storms for Ice-Free and Ice-Covered
555 Lake Erie, *J. of Coastal Research*, 33(6), 1383-1396, <https://doi.org/10.2112/JCOASTRES-D-16-00101.1>, 2017.
- 557 FEMA: FEMA Great Lakes Coastal Guidelines, Appendix D.3 Update. FEMA, 2014.
- 558 Forbes, C., Luettich, R.A., Mattocks, C.A., and Westerink, J.J.: A retrospective evaluation of the storm
559 surge produced by Hurricane Gustav (2008): Forecast and hindcast results, *Wea. Forecasting*,
560 25(6), 1577–1602, <https://doi.org/10.1175/2010WAF2222416.1>, 2010.
- 561 Fleming, J.G., Fulcher, C.W., Luettich Jr., R.A., Estade, B.D., Allen, G., and Winer, H.S.: A real time storm
562 surge forecasting system using ADCIRC, *Proceedings of the International Conference on Estuarine*
563 *and Coastal Modeling*, [https://doi.org/10.1061/40990\(324\)48](https://doi.org/10.1061/40990(324)48), 2008.
- 564 Gallagher, G.W., Duncombe, R.K., and Steeves, T. M.: Establishing Climate Change Resilience in the
565 Great Lakes in Response to Flooding, *Journal of Science Policy & Governance*, 17(1),
566 <https://doi.org/10.38126/JSPG170105>, 2020.
- 567 Gronewold, A.D., and Rood, R.B.: Recent water level changes across Earth’s largest lake system and
568 implications for future variability, *J. of Great Lakes Research*, 45(1), 1-3,
569 <https://doi.org/10.1016/j.jglr.2018.10.012>, 2019.
- 570 Gronewold, A.D., Fortin, V., Lofgren, B., Clites, A., Stow, C.A., and Quinn, F.: Coasts, water levels, and
571 climate change: A Great Lakes perspective, *Climate Change*, 120, 697-711,
572 <https://doi.org/10.1007/s10584-013-0840-2>, 2013.



- 573 Huang, A., Rao, Y.R., Lu, Y., and Zhao, J.: Hydrodynamic modelling of Lake Ontario: An intercomparison
574 of three models. *Journal of Geophysical Research: Oceans*, 115(C12), 1-16,
575 <https://doi.org/10.1029/2010JC006269>, 2010.
- 576 Kelley, J.G.W., Chen, Y., Anderson, E.J., Lang, G.A., and Xu, J.: Upgrade of NOS Lake Erie Operational
577 Forecast System (LEOFS) to FVCOM: Model Development and Hindcast Skill Assessment; NOS
578 CS 40, NOAA; NOAA Technical Memorandum, <http://doi.org/10.7289/V5/TM-NOS-CS-40>,
579 2018.
- 580 Lesser, G.R., Roelvink, J.A., and Stelling, G.S.: Development and validation of a three-dimensional
581 morphological model, *Coastal Engineering*, 51(8-9), 883-915,
582 <https://doi.org/10.1016/j.coastaleng.2004.07.014>, 2004.
- 583 Lin, S., Boegman, L., Shan, S., and Mulligan, R.P.: An automatic lake-model application using near real-
584 time data forcing: Development of an operational forecast workflow (COASTLINES) for Lake
585 Erie, *Geosci. Model Dev*, 15(3), 1331-1353, <https://doi.org/10.5194/gmd-15-1331-2022>, 2022.
- 586 McCombs, M.P., Mulligan, R.P., Boegman, L., and Rao, Y.R.: Modelling surface waves and wind-driven
587 circulation in eastern Lake Ontario during winter storms, *J. Great Lakes Res.*, 40(3), 130-142,
588 <https://doi.org/10.1016/j.jglr.2014.02.009>, 2014a.
- 589 McCombs, M.P., Mulligan, R.P., and Boegman, L.: Offshore wind farm impacts on surface waves and
590 circulation in Eastern Lake Ontario, *Coastal Engineering*, 93, 32-39,
591 <https://doi.org/10.1016/j.coastaleng.2014.08.001>, 2014b.
- 592 Mao, M., and Xia, M.: Dynamics of wave-current-surge interactions in Lake Michigan: A model
593 comparison, *Ocean Modelling*, 110, 1-20, <https://doi.org/10.1016/j.ocemod.2016.12.007>, 2007.
- 594 Milbrandt, J.A., Belair, S., Faucher, M., Vallee, M., Carrera, M.L., and Glazer, A.: The Pan-Canadian High
595 Resolution (2.5 km) Deterministic Prediction System, *Weather and Forecasting*, 31(6), 1791-1816,
596 <https://doi.org/10.1175/WAF-D-16-0035.1>, 2016.
- 597 Oveisy, A., Boegman, L., and Imberger, J.: Three-dimensional simulation of lake and ice dynamics during
598 winter, *Limnol Oceanogr*, 57(1), 43-57, <https://doi:10.4319/lo.2012.57.1.0043>, 2012.
- 599 Paramygin, V.A., Sheng, Y.P., and Davis, J.R.: Towards the development of an operational forecast system
600 for the Florida coast, *J. Mar. Sci. Eng.*, 5(1), <https://doi.org/10.3390/jmse5010008>, 2017.
- 601 Paturi, S., Boegman, L., and Rao, Y.R.: Hydrodynamics of eastern Lake Ontario and the upper St. Lawrence
602 River, *J. Great Lakes Res.*, 38(4), 194-204, <https://doi.org/10.1016/j.jglr.2011.09.008>, 2012.
- 603 Peng, M., Zhang, A., Anderson, E.J., Lang, G.A., Kelley, J.G.W., and Chen, Y.: Implementation of the
604 Lakes Michigan and Huron Operational Forecast System (LMHOFS) and the Nowcast/Forecast
605 Skill Assessment, NOAA technical report NOS CO-OPS, 2019.



- 606 Prakash, S., Atkinson, J.F., and Green, M.L.: A semi-Lagrangian study of circulation in Lake Ontario, J.
607 Great Lakes Res., 33(4), 774-790,
608 [https://doi.org/10.3394/0380-1330\(2007\)33\[774:ASSOCA\]2.0.CO;2](https://doi.org/10.3394/0380-1330(2007)33[774:ASSOCA]2.0.CO;2), 2007.
- 609 Rey, A.J.M., and Mulligan, R.P.: Influence of hurricane wind field variability on real-time forecast
610 simulations of the coastal environment, Journal of Geophysical Research: Oceans, 126(1), 1-20,
611 <https://doi.org/10.1029/2020JC016489>, 2021.
- 612 Shore, J.A.: Modelling the circulation and exchange of the Kingston Basin and Lake Ontario with FVCOM,
613 Ocean Modelling, 30(2-3), 106-114, <https://doi.org/10.1016/j.ocemod.2009.06.007>, 2009.
- 614 Sogut, D.V., Jensen, R.E., and Farhadzadeh, A.: Characterizing Lake Ontario Marine Renewable Energy
615 Resources, Marine Technology Society Journal, 53(2), 21-38,
616 <https://doi.org/10.4031/MTSJ.53.2.3>, 2019.
- 617 Steinschneider, S.: A hierarchical Bayesian model of storm surge and total water levels across the Great
618 Lakes shoreline – Lake Ontario, J. Great Lakes Res. 47(3), 829-843,
619 <https://doi.org/10.1016/j.jglr.2021.03.007>, 2021.
- 620 Studholme, J., Fedorov, A.V., Gulev, S.K., Emanuel, K., and Hodges, K.: Poleward expansion of tropical
621 cyclone latitudes in warming climates, Nature geoscience, 15, 14-18,
622 <https://doi.org/10.1038/s41561-021-00859-1>, 2022.
- 623 Swatridge, L.L., Mulligan, R.P., Boegman, L., Shan, S., and Valipour, R.: Coupled modelling of storm
624 surge, circulation, and surface waves in a large, stratified lake, J. Great Lakes Res, 48(6), 1520-
625 1535, <https://doi.org/10.1016/j.jglr.2022.08.023>, 2022.